

*Citation for published version:*

Pelecanos, L, Kontoe, S & Zdravkovic, L 2017, 'Steady-state and transient dynamic visco-elastic response of concrete and earth dams due to dam-reservoir interaction', Paper presented at 6th International Conference on Computational Methods in Structural Dynamics and Earthquake Engineering, Rhodes, Greece, 15/06/17 - 17/06/17.

*Publication date:*  
2017

[Link to publication](#)

**University of Bath**

**Alternative formats**

If you require this document in an alternative format, please contact:  
[openaccess@bath.ac.uk](mailto:openaccess@bath.ac.uk)

**General rights**

Copyright and moral rights for the publications made accessible in the public portal are retained by the authors and/or other copyright owners and it is a condition of accessing publications that users recognise and abide by the legal requirements associated with these rights.

**Take down policy**

If you believe that this document breaches copyright please contact us providing details, and we will remove access to the work immediately and investigate your claim.

## STEADY-STATE AND TRANSIENT DYNAMIC VISCO-ELASTIC RESPONSE OF CONCRETE AND EARTH DAMS DUE TO DAM- RESERVOIR INTERACTION

Loizos Pelecanos<sup>1</sup>, Stavroula Kontoe<sup>2</sup>, and Lidija Zdravković<sup>2</sup>

<sup>1</sup>Department of Architecture & Civil Engineering, University of Bath,  
Claverton Down, Bath, BA2 7AY, United Kingdom.  
e-mail: L.Pelecanos@bath.ac.uk

<sup>2</sup> Department of Civil & Environmental Engineering, Imperial College London  
Skempton Building, Exhibition Road, London, SW7 2AZ, United Kingdom  
{stavroula.kontoe, l.zdravkovic}@imperial.ac.uk

**Keywords:** Dam, Reservoir, Interaction, Earthquake Engineering, Finite elements, Structural Dynamics.

**Abstract.** *The aim of this study is to investigate the effects of dam–reservoir interaction on the dynamic response of dams. Both thin rectangular concrete cantilever and large trapezoidal earth dams are considered with empty and full reservoir.*

*It has recently been shown by Pelecanos et al. [32] that the amplification of accelerations at the crest of the dam depends on the combinations of the frequency of the harmonic acceleration load and the fundamental frequencies of the dam and the reservoir. This study considers transient dynamic loading and selected scenarios of different combinations of the above-mentioned frequencies are examined under random seismic acceleration load.*

*It is shown that for certain cases the amplification of accelerations of the dam can be affected by the presence of the upstream reservoir. In general, thin rectangular concrete cantilever dams are found to be considerably more sensitive to dam–reservoir interaction than large trapezoidal earth dams. Therefore, this investigation examines the significance of dam–reservoir interaction and when this interaction should be taken into consideration or it could be neglected.*

## 1 INTRODUCTION

The dynamic behaviour of a dam with a full reservoir is different from the behaviour of a dam with an empty reservoir. The motion of the reservoir affects the motion of the dam (because of the induced hydrodynamic pressures [7, 8]) and vice-versa. This phenomenon is called dynamic dam-reservoir interaction (DRI) and it could be catastrophic in cases of resonance, i.e. when the two domains (dam and reservoir) are vibrating in phase.

The early studies on the effects of the reservoir on the response of dams considered a stiff and undeformable dam of various geometries [40, 39, 41, 2, 5] and concentrated on the prediction of the hydrodynamic pressures on the upstream dam face [28, 11, 12, 26]. Later studies considered a flexible dam [7, 25] and investigated the vibrations of both the reservoir and the dam structure. Over time various closed-form analytical solutions were proposed [40, 41, 6] for simplified problems, while more advanced numerical models [32, 18, 40] were adopted to consider the complicated interaction between the dam and the reservoir by discretising both domains. The latter were generally based on Finite [16, 34, 30] and/or Boundary Element [38] approaches.

Previous studies of DRI [5, 7, 17, 21, 20, 19] showed that the effects of DRI are more pronounced in concrete dams than in earth dams. For this reason, seismic analyses of earth dams have traditionally neglected DRI effects [31]. The early fundamental work of Chopra [7] is of particular interest, as it studied a model concrete gravity dam vibrating in its fundamental mode and examined its response for various combinations of the circular frequency of the applied harmonic load and the fundamental circular frequencies of the dam and the reservoir. The effects of this interaction are mainly focused on (a) the fundamental period of vibration of the dam-reservoir system (DRS) and (b) the magnitude of the dynamic response of the dam. It is generally believed that DRI firstly causes the DRS to soften, elongating its fundamental period of vibration, and secondly it alters the dam's response by amplifying or de-amplifying the seismic motion. Finally, monitoring data from forced vibration tests on real concrete gravity dams [8] showed that the measured natural period of vibration of dams was larger for a full reservoir than a partly filled reservoir [9, 15, 16, 35].

A recent study by Pelecanos et al. [32] investigated the fundamental behavior of dam-reservoir systems under harmonic loads and examined the amplification of accelerations at steady-state conditions. Two general cases were considered of simplified model concrete cantilever and trapezoidal earth. The amplification of accelerations at the crest of the dam was explored under harmonic acceleration load for various combinations of the frequency of the harmonic load and the fundamental frequencies of the dam and the reservoir. It was found that DRI affects both the fundamental period of the dam and the amplification of accelerations within the dam structure and that these DRI effects are more pronounced for concrete cantilever dams than trapezoidal earth dams.

This paper describes a further investigation of reservoir-dam interaction and its influence on the dynamic acceleration response of dams. It builds on the work of Pelecanos et al. [32] and extends that work to transient dynamic acceleration loads by considering seismic input motions. Similar to the study of Pelecanos et al. [32], both rectangular cantilever and trapezoidal earth dams are considered. In all the performed analyses, both the dam and the reservoir rest on a stiff undeformable ground and therefore the effects of dam-reservoir-foundation interaction are not considered.

## 2 PROBLEM DEFINITION

The problem under study is shown in Figure 1. A dam (1) rests on the ground (in this work, a stiff and undeformable foundation) (3) and retains a large amount of water in the reservoir

(2). Under seismic (or general dynamic) conditions, an acceleration motion from the ground (such as at point A) causes movement of both the dam structure and the reservoir.

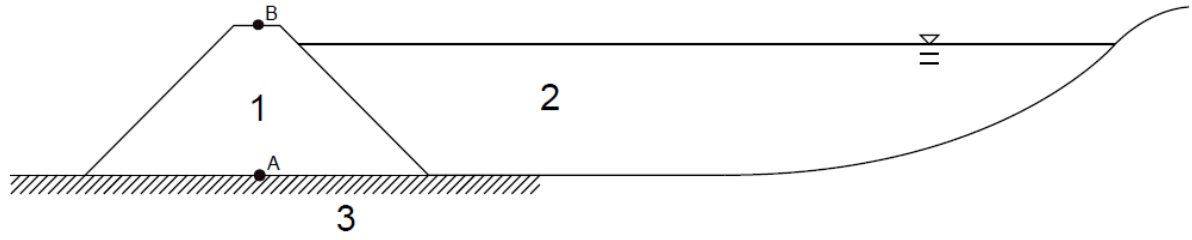


Figure 1: Geometry of the dam-reservoir-foundation system: (1) Dam, (2) Reservoir, (3) Foundation.

The critical question is how the motion of each domain (dam structure and reservoir) will be affected by the motion of the neighbouring domain, i.e. what is the effect of reservoir-dam interaction, especially on the accelerations of the dam crest (point B). Therefore, in this investigation, acceleration input motions are applied at the dam base (such as point A) and the accelerations at the crest of the dam (point B) are monitored and examined for different cases, with a full and an empty reservoir.

In all the analyses presented in this paper, the reservoir domain is modelled with 8-noded isoparametric displacement-based solid elements according as elaborated in Pelecanos et al. [30]. All the analyses carried out are two-dimensional plane-strain dynamic in the time-domain using the FE software ICFEP (Imperial College Finite Element Program) [33]. The time-integration scheme employed is the generalised  $\alpha$ -method of Chung & Hulbert [10] which is able to use numerical damping to selectively filter high frequencies (spectral radius at infinity,  $\rho_\infty = 9/11$ , see Kontoe et al. [23]).

### 3 FINITE ELEMENT MODELS

#### 3.1 Rectangular concrete dam

The first case considers a simple rectangular cantilever dam. The geometry of the cantilever dam is shown in Figure 2. The region A-B-C-D represents the upstream reservoir, A-B-F-E represents the cantilever dam and F-G-H-C represents the foundation. The height of the dam is taken as,  $H=60\text{m}$ , the width of the dam is  $W=18\text{m}$ , the length of the reservoir,  $L=300\text{m}$  and the thickness of the foundation,  $T=18\text{m}$ . The reservoir length to height ratio is taken as,  $L/H = 5$  according to the suggestions of Pelecanos et al. [30] for stiff dams with a vertical upstream face.

The material properties of the dam are taken as follows: Poisson's ratio,  $\nu=0.3$  and mass density,  $\rho=2500\text{ kg/m}^3$ . Damping,  $\xi$ , of the Rayleigh type [8] is specified in the dam with a target value of 5%. The values for the two natural circular frequencies of Rayleigh damping,  $\omega_1$  and  $\omega_2$ , are taken as equal to the fundamental circular frequency of the dam,  $\omega_d$ , and the circular predominant frequency of the input excitation  $\omega$ . The foundation is modelled as rigid and a high bulk modulus value is assigned,  $K = 10^8 K_w = 2.2 \cdot 10^{14}\text{ kPa}$  (where,  $K_w = 2.2 \cdot 10^6\text{ kPa}$  is the bulk modulus of water) and a Poisson's ratio  $\nu=0.4$ .

The reservoir water is assumed to behave as a linear material with a bulk modulus,  $K_w=2.2 \cdot 10^6\text{ kPa}$  (the exact value for water) and a nominal value of shear modulus,  $G_w=100\text{ kPa}$  [30]. The fundamental circular frequency of the reservoir,  $\omega_r$  is given by Equation 1 [5] (where,  $V_p=1483\text{ m/s}$  is the p-wave velocity of water).

$$\omega_r = 0.25 \frac{V_p}{H} \quad (1)$$

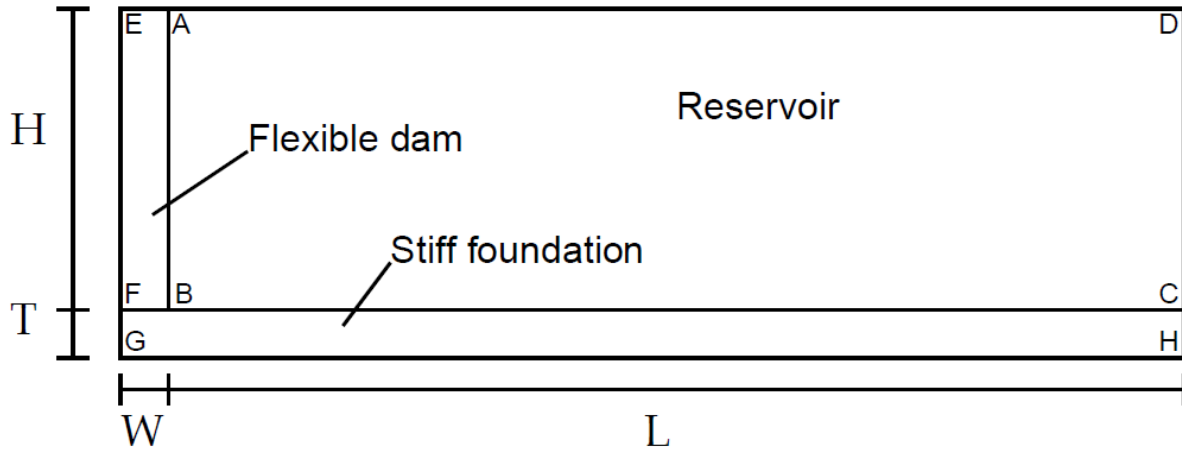


Figure 2: Geometry of the rectangular dam.

It should be noted that the value of the elastic Young modulus,  $E$ , is altered in each analysis so that specific combinations of  $\omega$ ,  $\omega_r$  and  $\omega_d$  are achieved. This is discussed in more detail in Section 5.1. The fundamental frequency of the dam may be obtained from the Euler-Bernoulli or Timoshenko bending equations [35].

Zero-thickness isoparametric interface elements [13][33] are placed along the interface of the dam and the reservoir (A-B) and the interface of the reservoir and the foundation (B-C). The values assigned for the normal and shear stiffness of the interface elements are  $K_N=10^8$  kN/m and  $K_S=1$  kN/m respectively [30].

The applied boundary conditions include: zero displacements in the vertical direction along the bottom boundary (G-H), and prescribed values of acceleration in the horizontal direction. Zero displacements are specified in the vertical direction on the upstream reservoir boundary, whereas the horizontal boundary condition applied on the upstream reservoir boundary (C-D) is the standard viscous boundary [22][24] which is described by Equation 2 [30].

$$\sigma = \rho V_p \dot{u} \quad (2)$$

where  $\sigma$  is a normal stress on the boundary,  $\rho$  is the density of the material the BC has been applied to (i.e. water in this case),  $V_p$  is the p-wave velocity of the water ( $=1483$  m/s) and  $\dot{u}$  is the velocity in the horizontal direction. More details about this BC may be found in Kontoe et al. [24].

### 3.2 Trapezoidal earth dam

The geometry of the examined earth dam is shown in Figure 3. The region A-B-C-D represents the upstream reservoir, A-B-F-E represents the earth dam and F-G-H-C represents the foundation. The height of the dam is taken as  $H=60$ m, the width of the crest of the dam  $W=18$ m, the breadth of the dam shoulders  $B=180$ m, the length of the reservoir  $L=300$ m and the thickness of the foundation  $T=18$ m. Note that the slope ratio,  $B/H = 1/3$ . The  $L/H$  ratio is taken as equal to 5 according to the suggestions of [30] for trapezoidal earth dams.

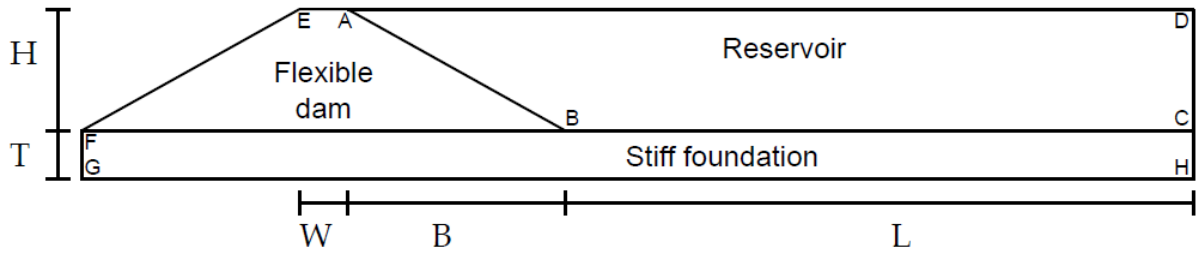


Figure 3: Geometry of the trapezoidal earth dam considered.

The material properties of the dam are as follows: Poisson's ratio,  $\nu=0.3$  and mass density,  $\rho=2000 \text{ kg/m}^3$ . Similarly to the cantilever dam, damping,  $\xi$  of the Rayleigh type [8] is specified in the dam with a target value of 5% and the foundation is again modelled to behave as a rigid material. The boundary conditions are the same as the cantilever dam case: zero displacements are specified in the vertical direction along the bottom boundary (G-H), whereas the acceleration input motion is specified in the horizontal direction.

The value of the shear wave velocity,  $V_s$ , is altered in each analysis so that specific combinations of  $\omega$ ,  $\omega_r$  and  $\omega_d$  are achieved. This is discussed in more detail in Section 5.2. The fundamental frequency of the dam may be obtained from the Ambraseys [1] equation [37].

Again, interface elements are placed at the interface of the dam and the reservoir (A-B) and the interface of the reservoir and the foundation (B-C). Finally, the same boundary conditions are applied on the bottom (F-G) and the upstream reservoir (C-D) boundaries as with the previous case of the cantilever dam.

#### 4 DAM-RESERVOIR INTERACTION UNDER HARMONIC LOADING

Pelecanos et al. [32] studied the response of both concrete cantilever and trapezoidal earth dams under harmonic loads. For both cases the amplification of accelerations at the crest of the dam was explored under harmonic acceleration load for various combinations of the frequency of the harmonic load,  $\omega$ , and the fundamental frequencies of the dam,  $\omega_d$ , and the reservoir,  $\omega_r$ . To achieve these different combinations, the values of the elastic modulus,  $E$ , and of the shear wave velocity,  $V_s$ , were altered in the case of the concrete cantilever dam and the trapezoidal earth dam respectively, to provide some specific values of the ratio of the fundamental circular frequency of the reservoir over the fundamental circular frequency of the dam,  $\omega_r/\omega_d$ , over the range of 0.25 to 4.

The applied boundary conditions included: zero displacements in the vertical direction along the bottom boundary (G-H), and prescribed values of harmonic acceleration in the horizontal direction, as given by Equation 3. Different values of circular frequency,  $\omega$ , were considered, for constant amplitude  $\alpha_0 = 1 \text{ m/s}^2$  and for 40 cycles, in order to reach a steady-state response.

$$\alpha(t) = \alpha_0 \cos \omega t \quad (3)$$

where,  $\alpha$  is the input acceleration,  $\alpha_0$  is the amplitude of the harmonic load,  $\omega$  is the circular frequency of the harmonic loading and  $t$  is the time.

Regarding the rectangular cantilever dam, Figure 4 (from Pelecanos et al. [32]) shows the amplification of the accelerations at the dam crest,  $|F|$  with respect to the ratio of the circular frequency of the harmonic load to the fundamental circular frequency of the dam,  $\omega/\omega_d$ , for various values of the ratio of the fundamental circular frequency of the reservoir to the fun-

damental circular frequency of the dam,  $\omega_r/\omega_d$ . On the same figure, the corresponding amplification of a dam with an empty reservoir is plotted with a dashed line for comparison.

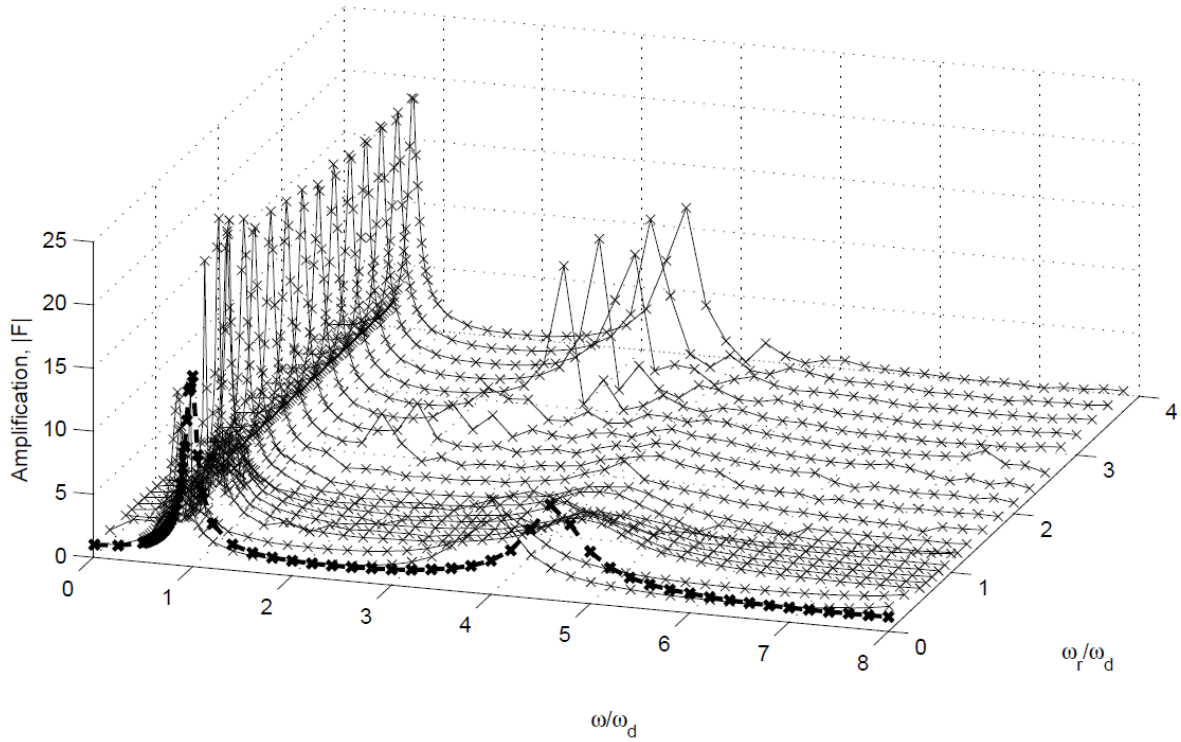


Figure 4: Amplification of acceleration,  $|F|$  at the crest of the rectangular concrete dam for various values of the frequency ratios  $\omega/\omega_d$  and  $\omega_r/\omega_d$  (After Pelecanos et al. [32]).

The amplification spectrum ( $|F|$  -  $\omega/\omega_d$ ) follows a similar trend for all the values of the examined  $\omega_r/\omega_d$  ratio. Namely, there are generally two peak values of the amplification as observed for the empty reservoir case. However, the magnitude of the peak values of the amplification and the value of the  $\omega/\omega_d$  ratio at which they occur is different for different values of the  $\omega_r/\omega_d$  ratio.

Moreover, it is shown that the maximum value of amplification occurs in the region where  $\omega/\omega_d \approx \omega_r/\omega_d \approx 1$ , i.e. where  $\omega \approx \omega_d \approx \omega_r$ . This is due to resonance between the harmonic load, the dam and the reservoir. There are also large values of amplification for  $\omega/\omega_d \approx \omega_r/\omega_d$  (shown diagonally in the figure), i.e. where  $\omega \approx \omega_r$ . The value of amplification for the latter case ( $\omega \approx \omega_r$ ) can be larger than the amplification corresponding to the second mode of vibration (i.e. close to  $\omega/\omega_d \approx 4.7$ ). However, it seems that in some cases (e.g. close to  $\omega/\omega_d \approx \omega/\omega_r \approx 3$ ) there is a combined effect of (a)  $\omega \approx \omega_r$  and (b) the second natural mode of vibration of the dam.

Regarding the trapezoidal earth dam, Figure 5 (from Pelecanos et al. [32]) shows the amplification of acceleration,  $|F|$ , at the dam crest with respect to the ratio of the circular frequency of the harmonic load to the fundamental circular frequency of the dam,  $\omega/\omega_d$  for various values of the ratio of the fundamental circular frequency of the reservoir to the fundamental circular frequency of the dam,  $\omega_r/\omega_d$ . The amplification of a dam with an empty reservoir is also plotted with a dashed line for comparison.



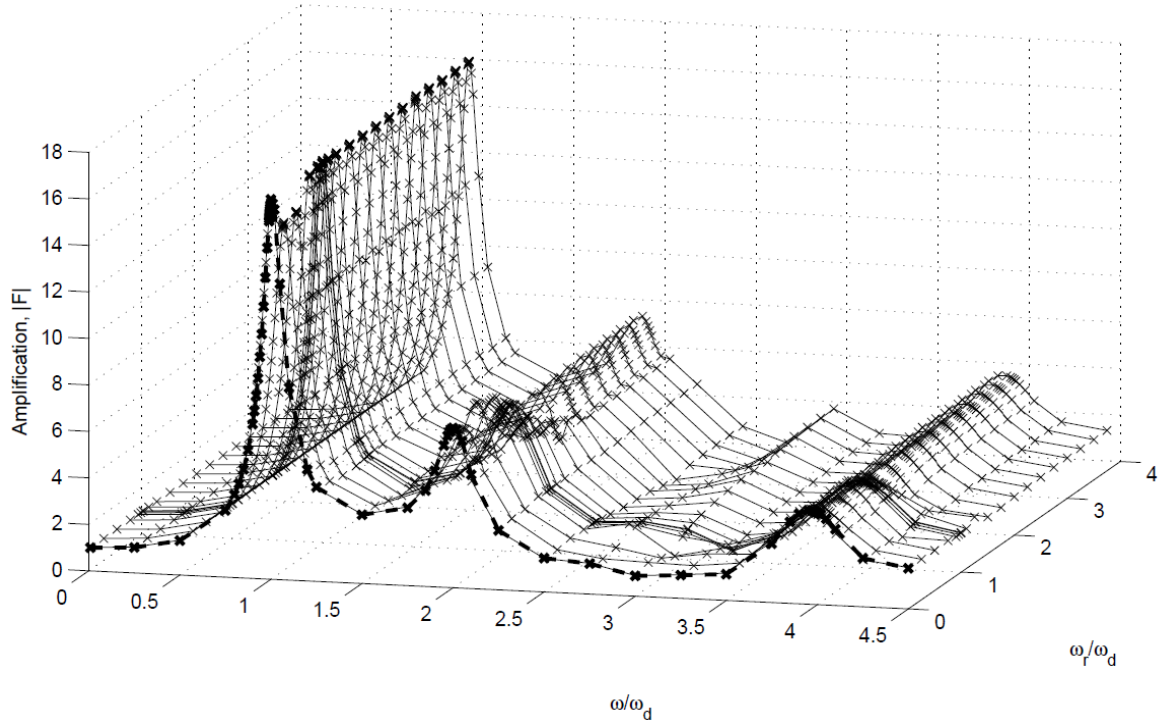


Figure 5: Amplification of acceleration,  $|F|$  at the crest of the earth dam for various values of the frequency ratios  $\omega/\omega_d$  and  $\omega_r/\omega_d$  (After Pelecanos et al. [32]).

Similar to the case of the cantilever dam, the amplification spectrum ( $|F| - \omega/\omega_d$ ) follows a similar trend for all the values of the  $\omega_r/\omega_d$  ratio. Namely, for each  $\omega_r/\omega_d$  ratio three main peaks can be identified in the amplification response, which correspond to the three first modes of vibration of the dam. In contrast to the case of the cantilever dam, the magnitude of the peak values of the amplification and the value of the  $\omega/\omega_d$  ratio at which they occur does not seem to depend significantly on the  $\omega_r/\omega_d$  ratio. Overall, there are very small differences between the amplification spectra for different values of the  $\omega_r/\omega_d$  ratio. This suggests that the presence of the reservoir does not affect significantly the amplification (and hence the dynamic response) of the dam, for any value of the  $\omega_r/\omega_d$  ratio.

## 5 DAM-RESERVOIR INTERACTION UNDER SEISMIC LOADING

The investigation of Pelecanos et al. [32] was restricted to a harmonic load shaking a dam-reservoir system. However, since in reality dams are subjected to transient shaking, this study is concerned with seismic loading of reservoir-dam systems. The horizontal acceleration record of the El Centro (Imperial Valley, 1940) earthquake is used as the input motion. The acceleration time history of this motion is shown in Figure 6, and the corresponding 5% damped response spectrum is shown in Figure 7. As it is shown in the latter figure, there are two distinct peaks of spectral acceleration,  $S_a$  for periods of 0.27s and 0.52s. The period for which the maximum value of  $S_a$  occurs is considered to be the dominant period of the seismic load and it is  $T_{EQ} = 0.52s$ .



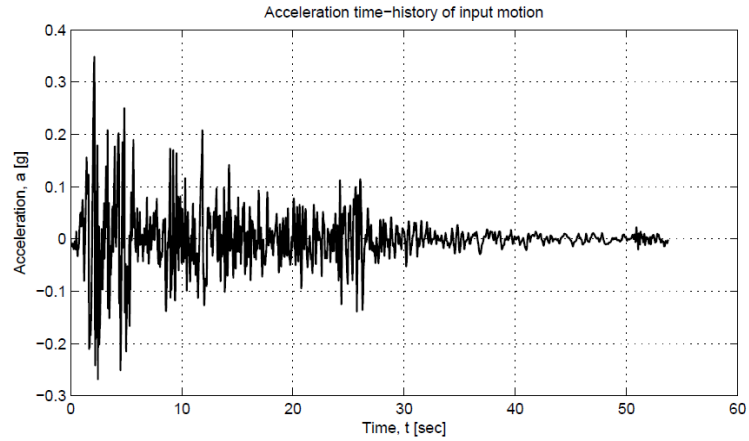


Figure 6: Acceleration time-history of the El-Centro (1940) earthquake record.

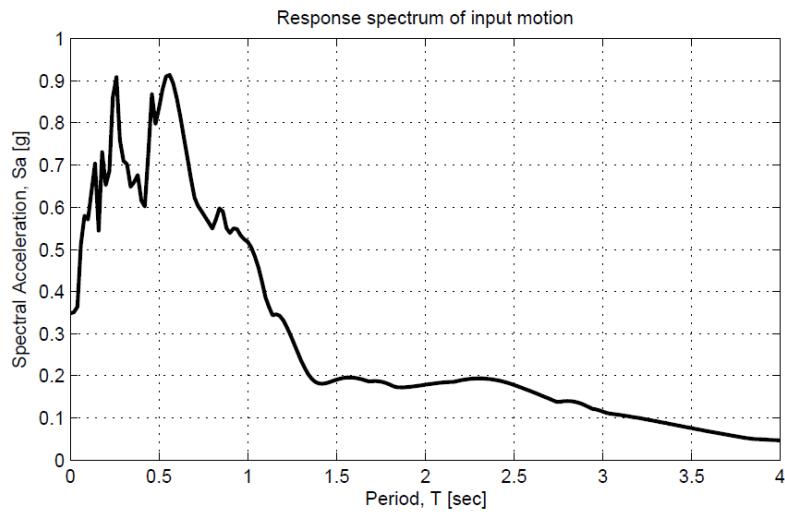


Figure 7: Response spectrum of the El Centro (1940) earthquake record for damping  $\xi=5\%$ .

Table 1: Cases of combinations of  $\omega/\omega_d$  and  $\omega_r/\omega_d$  frequency ratios examined for seismic loading.

CASE	$\omega/\omega_d$	$\omega_r/\omega_d$
A	1	1
B	3	3
C	1	3
D	1/3	1
E	1/3	1/3

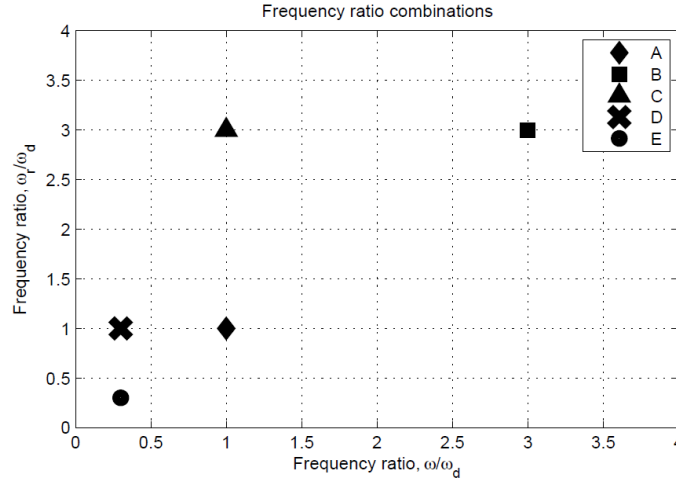


Figure 8: Cases of combinations of  $\omega/\omega_d$  and  $\omega_r/\omega_d$  frequency ratios examined under seismic loading.

Following the investigation of Pelecanos et al. [32] for harmonic loading, both a cantilever and a trapezoidal earth dam are again considered. For each of the dam types, five cases are examined for various combinations of the frequency ratios  $\omega/\omega_d$  and  $\omega_r/\omega_d$ , as listed in Table 1 and shown graphically in Figure 8. These combinations are chosen based on the observations of Pelecanos et al. [32] concerning harmonic loading, i.e. large amplification of accelerations is expected for Cases A-D, whereas smaller amplification of the accelerations is expected for Case E.

### 5.1 Rectangular concrete dam

For the case of the cantilever dam, the model geometry shown in Figure 2 is employed. The imposed boundary conditions are described in Section 3.1. All five cases (Table 2) are analysed twice, with a full and an empty reservoir. In all cases, the elastic modulus,  $E$ , is varied for each case as listed in Table 2, to achieve the combinations of frequencies listed in Table 1.

Table 2: Material and geometric properties of the rectangular concrete dam cases considered under seismic loading.

CASE	Height, $H$	Thickness, $t$	Elastic modulus, $E$
	[m]	[m]	[kPa]
A	180	18	$1.2 \cdot 10^9$
B	180	18	$1.4 \cdot 10^8$
C	60	6	$1.4 \cdot 10^8$
D	60	6	$1.2 \cdot 10^9$
E	180	18	$1.2 \cdot 10^{10}$

Figure 9 shows the acceleration time-histories at the crest of the dam (for both full and empty reservoirs), whereas Figure 10 shows the corresponding 5% damped response spectra. For the dam with a full reservoir and for all 5 cases (A, B, C, D and E), the peak value of amplification occurs at a value of the  $\omega/\omega_d$  ratio smaller than the corresponding for the dam with an empty reservoir (see Figure 10). This suggests that the fundamental period of the dam is larger when reservoir-dam interaction is considered. The latter conclusion is in agreement with the earlier observation of Pelecanos et al. [32] (see also Figure 4) for harmonic load, i.e. the load resonates with the dam-reservoir system at a smaller value of natural circular frequency,

therefore the fundamental period of the dam-reservoir system (i.e. dam with a full reservoir) is larger than that of a dam with an empty reservoir.

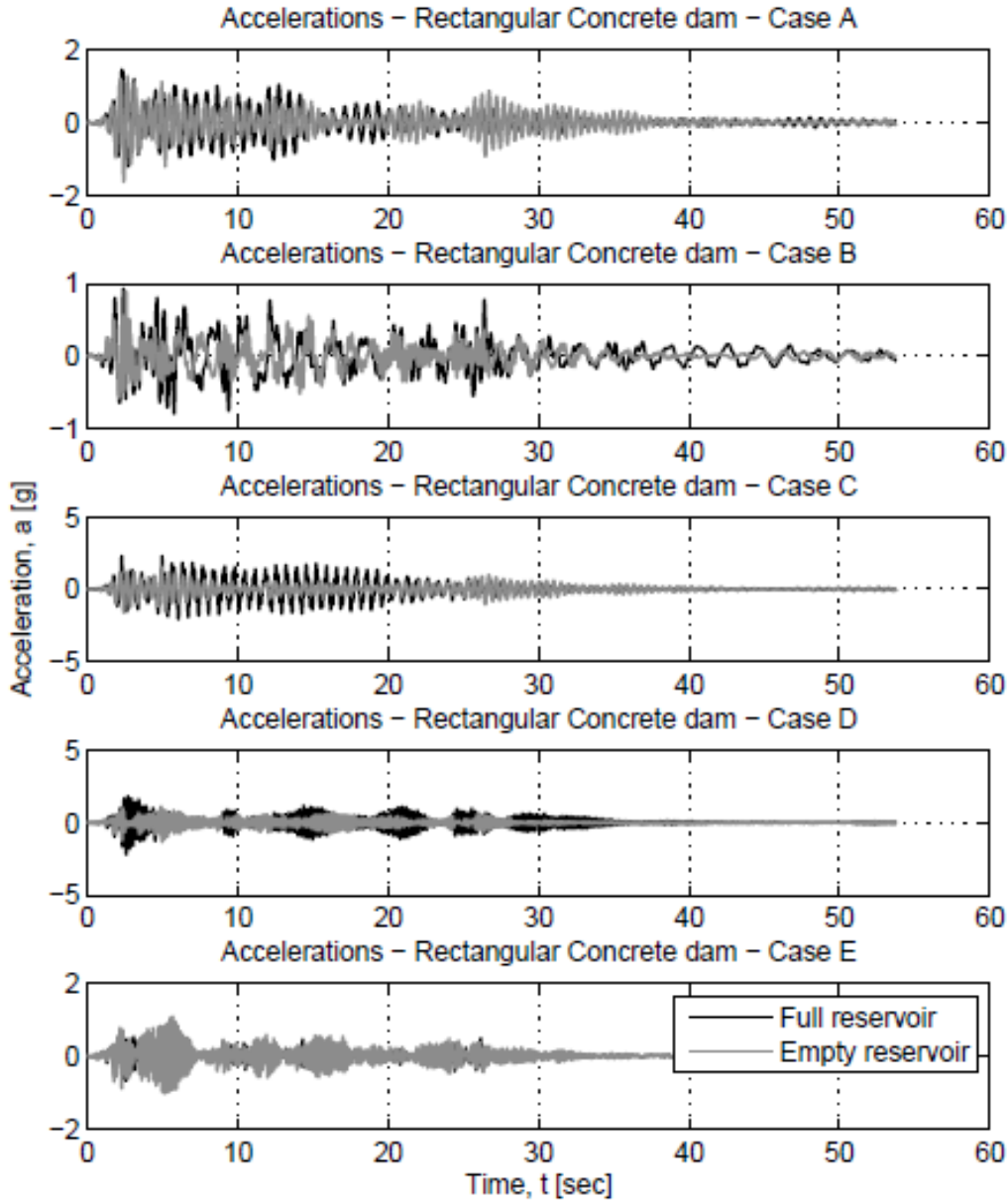


Figure 9: Acceleration time-histories at the crest of the rectangular concrete dam.

Moreover, the value of amplification of accelerations is larger for cases A-D with a full reservoir than those with an empty reservoir (Figure 10). This is again in agreement to the investigation of Pelecanos et al. [32] using harmonic loading (see Figure 4), where higher values of amplification were observed for the frequency combinations of cases A-D for the dam with a full reservoir.

Besides, for case E (i.e. for  $\omega/\omega_d = \omega_r/\omega_d = 1/3$ ), the amplification of accelerations is found to be smaller for a dam with a full reservoir than that for a dam with an empty reservoir (Figure 10). This is again in agreement with the previous investigation regarding harmonic loading (see Figure 4), where the amplification for  $\omega/\omega_d = \omega_r/\omega_d = 1/3$  was smaller in a dam with a full reservoir than a dam with an empty reservoir.

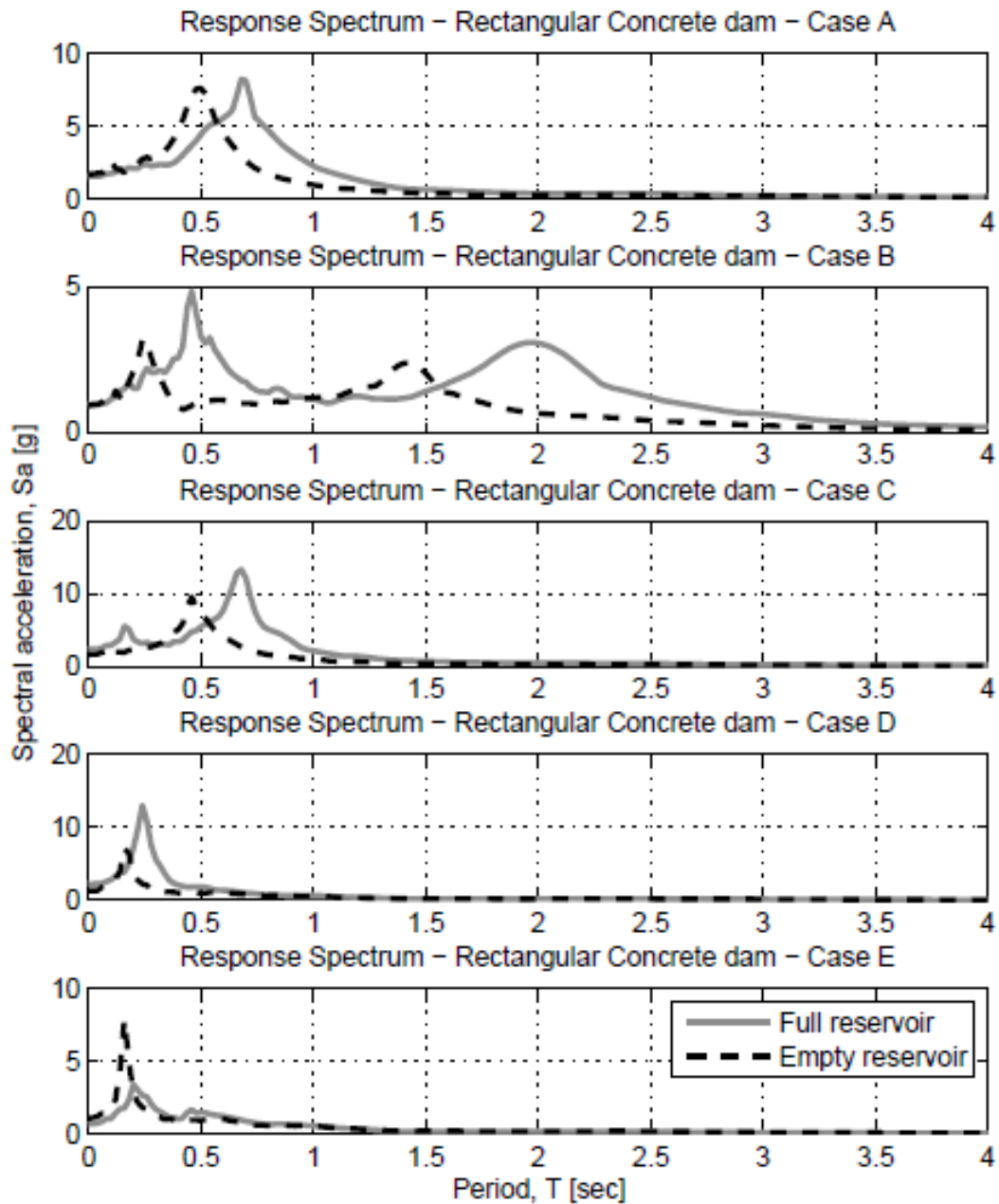


Figure 10: Response spectra (for damping  $\xi=5\%$ ) of the acceleration at the crest of the rectangular concrete dam.

## 5.2 Trapezoidal earth dam

For the case of the earth dam, the model geometry shown in Figure 3 is employed. The boundary conditions imposed are described in Section 3. Again, all five cases (Table 1) are analysed twice, with a full and empty reservoir. The shear wave velocity,  $V_s$ , is changed in each case as listed in Table 3, to achieve the combinations of frequencies listed in Table 1, but in all cases keeping the value of the p-wave velocity of the reservoir constant,  $V_p = 1483$  m/s.

Table 3: Material and geometric properties of the trapezoidal earth dam cases considered under seismic loading.

CASE	Height, H [m]	Shear wave velocity, $V_s$ [m/s]
A	900	4500
B	900	1500
C	300	1500
D	300	4500
E	900	13500

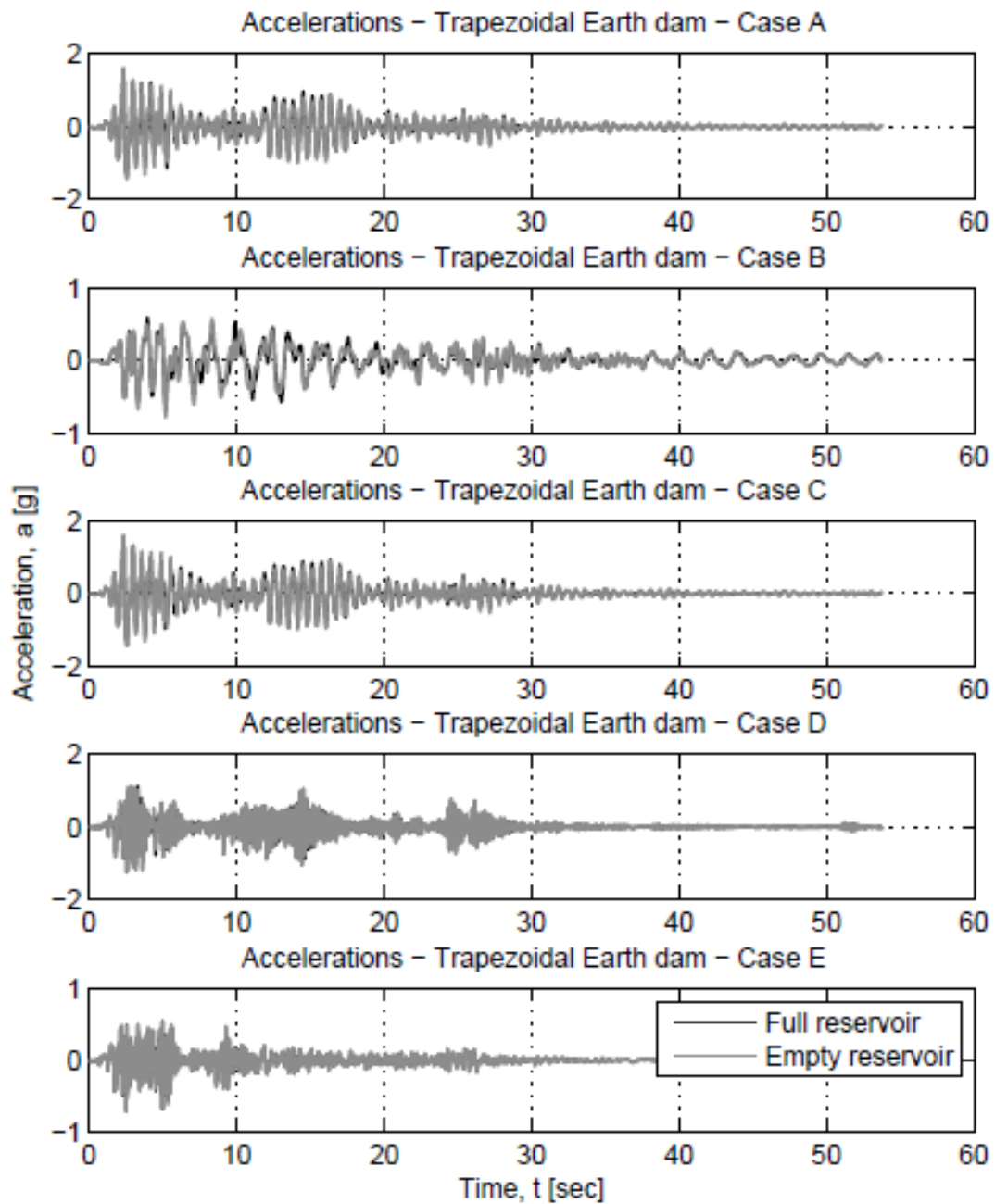


Figure 11: Acceleration time-histories at the crest of the earth dam.

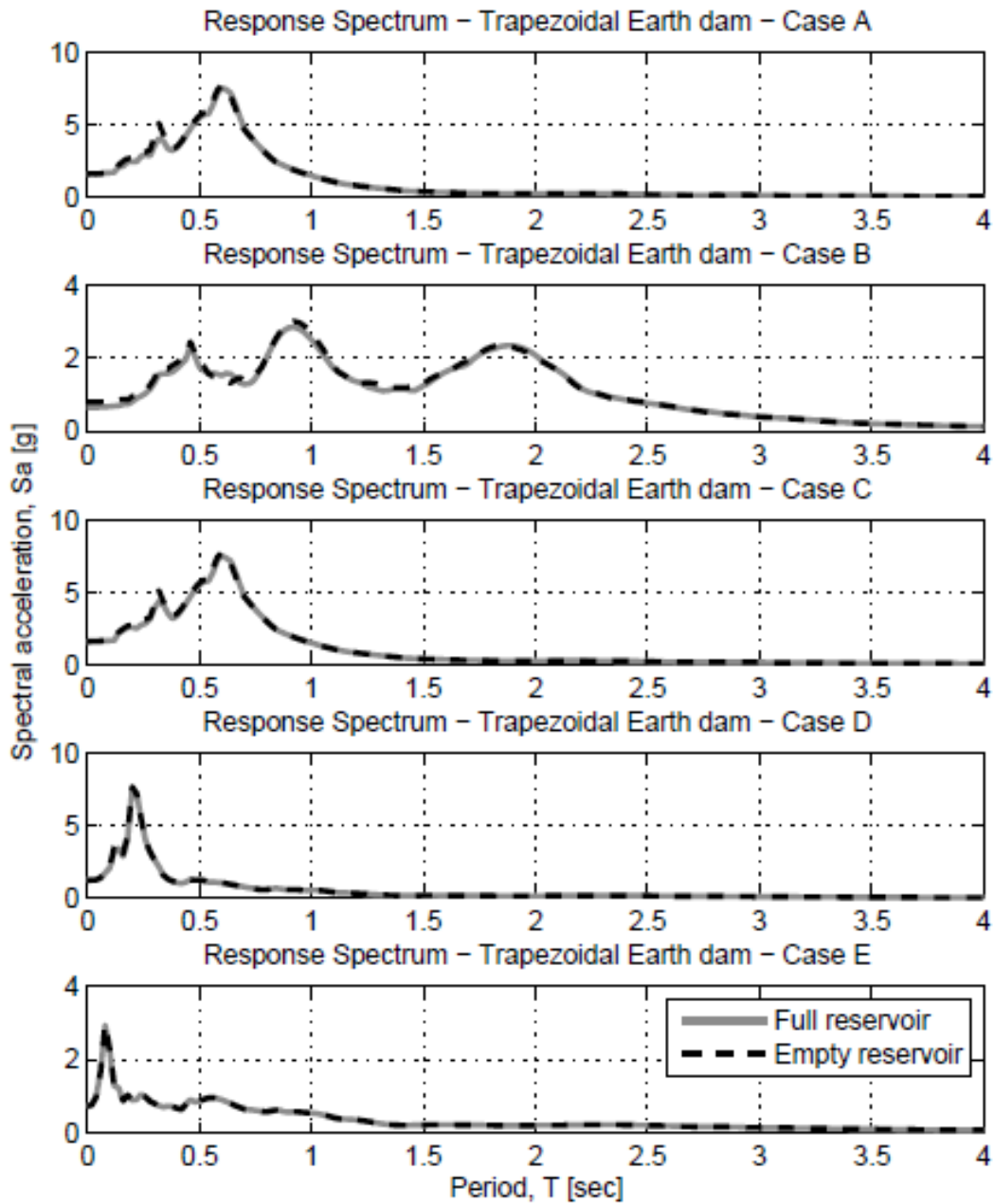


Figure 12: Response spectra (for damping  $\xi=5\%$ ) of the acceleration at the crest of the earth dam.

Figure 11 shows the acceleration time-histories at the crest of the dam (for both full and empty reservoirs), whereas Figure 12 show the corresponding 5% damped response spectra. It may be observed from all figures that the observations for the cantilever dam case do not apply to the earth dam. Although some minor differences between the full and empty reservoir cases may be noticed in the acceleration time-histories (Figure 11), no major differences exist in the response spectra (Figure 12). This means that both the frequency content and the value of amplification are not significantly affected by the presence of the reservoir, for all cases A-E, i.e. for various combinations of the frequency ratios. The previous conclusion of the negligible influence of the reservoir on the dynamic response of earth dams under harmonic loading from Pelecanos et al. [32] is therefore confirmed for seismic loading case as well.

The effects of DRI (both softening and amplification) are found to be insignificant for earth dams. This may be attributed to (a) the sloped upstream face and (b) the large volume of an earth dam. The hydrodynamic pressures induced on a sloped upstream dam face are smaller than those on a vertical dam face [42]. Moreover, the inertial effects from the additional mass from the reservoir are small compared to the inertia of a large earth dam. The second peak value of  $S_a$  did not affect the results of this section, as no resonance was expected for the cases chosen.

## 6 CONCLUSIONS

This paper describes an investigation carried out to assess the effects of reservoir-dam interaction on the transient dynamic (seismic) behaviour of dams. The main aim is to examine whether the presence of an upstream reservoir alters the response of a dam and to identify the cases in which the dynamic reservoir-dam interaction may have detrimental effects. Both rectangular cantilever and trapezoidal homogeneous earth dams are considered under seismic loading. This study is an extension of the work of Pelecanos et al. [32] who considered harmonic loads of a wide range of frequencies. The main conclusions of this study may be summarised as follows:

- The effects of dam-reservoir interaction (DRI) under seismic load are very similar to the DRI effects under harmonic loads at steady-state and therefore this study confirms the findings of Pelecanos et al. [32].
- The effects of DRI are mainly related to (a) change of the fundamental period of the dam and (b) change in the amplification of accelerations within the dam structure.
- DRI effects, in terms of both amplification of accelerations and change in the fundamental period, are more pronounced for cantilever dams. This could have an application on various water retaining structures with a slender cross-sectional geometry, such as arch dams, canal locks etc.
- Generally, the presence of the reservoir “softens” the response of the dam, i.e. it results in a larger fundamental period,  $T_d$  of the dam. This may be attributed to the added mass,  $m$  (see also Westergaard [40]) of the reservoir which vibrates with the dam. In contrast, the reservoir does not provide any additional (shear or bending) stiffness,  $k$  to the dam ( $T_d = 2\pi\sqrt{(m/k)}$ ).
- The amplification of the input acceleration in a dam with a reservoir can be either higher or lower than the amplification in a dam with an empty reservoir. This depends on the relative magnitude of the dominant circular frequency of the load,  $\omega$ , and the fundamental circular frequencies of the dam and reservoir,  $\omega_d$  and  $\omega_r$  respectively.

## ACKNOWLEDGEMENTS

This work was part of the PhD research of the first author at Imperial College London, funded by EPSRC. This support is gratefully appreciated. The assistance of Dr M. Latheef and Ms E. Skiada in the numerical analyses is also acknowledged.

## REFERENCES

- [1] Ambraseys, N. N., 1960, On the shear response of a two-dimensional truncated wedge subjected to arbitrary disturbance, *Bull. Seism. Soc. Am.*, 50, 1, 45-56.



- [2] Bustamante, J. I., Rosenblueth, E., Herrera, I., Flores, A., 1963, Presion hidrodinamica en presas y depositos. Boletin Sociedad Mexicana de Ingenieria Sismica, 1, 2.
- [3] Calcina, S. V., Eltrudis, L., Piroddi, L., Ranieri, G., 2014, Ambient Vibration Tests of an Arch Dam with Different Reservoir Water Levels: Experimental Results and Comparison with Finite Element Modelling, The Scientific World Journal, 692709, 1-12.
- [4] Chopra, A. K., 1966, Earthquake effects on dams, PhD Thesis, University of California, Berkeley.
- [5] Chopra, A. K., 1967, Earthquake response of earth dams, J. Soil Mech. Found. Div., ASCE, 93, SM2, 1399-1412.
- [6] Chopra, A. K., 1967, Hydrodynamic pressures on dams during earthquakes, J. Engrg. Mech. Div., ASCE, 93, EM6, 205-223.
- [7] Chopra, A. K., 1968, Earthquake behavior of reservoir-dam systems, J. Engrg. Mech. Div., ASCE, 94, EM6, 1475-1500.
- [8] Chopra, A. K., 1995, Dynamics of structures: Theory and application to earthquake engineering, Prentice-Hall, New Jersey.
- [9] Chopra, A. K., Gupta, S., 1978, Hydrodynamic and foundation interaction effects in frequency response functions for concrete gravity dams, Earthq. Engrg. and Struct. Dyn., 10, 1, 89-106.
- [10] Chung, J., Hulbert, G. M., 1993, A time integration algorithm for structural dynamics with improved numerical dissipation: the generalised- $\alpha$  method, J. Appl. Mech., 60, 371-375.
- [11] Chwang, A. T., 1978, Hydrodynamic pressures on sloping dams during earthquakes. Part 2: Exact theory, J. Fluid Mech., 87, 2, 343-348.
- [12] Chwang, A. T., Housner, G. W., 1978, Hydrodynamic pressures on sloping dams during earthquakes. Part 1. Momentum method, J. Fluid Mech., 87, 2, 335-341.
- [13] Day, R. A., Potts, D. M., 1994, Zero thickness interface elements - Numerical stability and application, Int. J. for Num. Anal. Meth. Geomech., 18, 10, 689-708.
- [14] Darbre, G. R., de Smet, C. A. M., Kraemer, C., 2000, Natural frequencies measured from ambient vibration response of the arch dam of Mauvoisin, Earthquake Engng. Struct. Dyn., 29, 5, 577-586.
- [15] Duron, Z. H., Hall, J. F., 1988, Experimental and finite element studies of the forced vibration response of morrow point dam, Earthq. Engrg. and Struct. Dyn., 16, 7, 1021-1039.
- [16] Fenves, G. L., Mojtahedi, S., Reimer, R. B., 1992, Effect of contraction joints on earthquake response of an arch dam, J. Struct. Engrg, ASCE, 118, 4, 1039-1055.
- [17] Hall, J. F., Chopra, A. K., 1980, Dynamic response of embankment, concrete-gravity and arch dams including hydrodynamic interaction, Earthquake Engineering Research Centre, University of California, Berkeley, EERC-80/39.
- [18] Hall, J. F., Chopra, A. K., 1982, Two-dimensional dynamic analysis of concrete gravity and embankment dams including hydrodynamic effects, Earthq. Engrg. and Struct. Dyn., 10, 2, 305-332.
- [19] Hall, J. F., Chopra, A. K., 1982, Hydrodynamic effects in earthquake response of embankment dams, J. Geotech. Engrg. Div., ASCE, 108, GT4, 591-597.
- [20] Hall, J. F., Chopra, A. K., 1982, Hydrodynamic effects in the dynamic response of concrete gravity dams, Earthq. Engrg. and Struct. Dyn., 10, 2, 333-345.
- [21] Hall, J. F., Chopra, A. K., 1982, Hydrodynamic effects in earthquake response of embankment dams, J. Geotech. Engrg. Div., ASCE, 108, GT4, 591-597.
- [22] Kellezi, L. X., 2000, Local transmitting boundaries for transient elastic analysis, Soil Dyn. and Earthq. Engrg., 19, 7, 533-547.
- [23] Kontoe, S., Zdravkovic, L., Potts, D.M., 2008, An assessment of time integration schemes for dynamic geotechnical problems, Comput. And Geotech., 2008, 35, 253-264.

- [24] Kontoe, S., Zdravkovic, L., Potts, D. M., 2009, An assessment of the domain reduction method as an advanced boundary condition and some pitfalls in the use of conventional absorbing boundaries, *Int. J. for Num. Anal. Meth. Geomech.*, 33, 309-330.
- [25] Lee, G. C., Tsai, C.S., 1991, Time domain analyses of dam-reservoir system. Part I: exact solution, *J. Engrg. Mech. Div., ASCE*, 117, 9, 1990-2006.
- [26] Liu, P. L. F., 1986, Hydrodynamic pressures on rigid dams during earthquakes, *J. Fluid Mech.*, 165, 131-145.
- [27] Lysmer, J., Kuhlemeyer, R. L., 1969, Finite dynamic model for infinite media, *J. Engrg. Mech. Div., ASCE*, 95, 4, 859-877.
- [28] Newmark, N. M., Rosenblueth, E., 1971, *Fundamentals of Earthquake Engineering*, Prentice-Hall Inc., Englewood Cliffs, New Jersey.
- [29] Pelecanos, L., 2013, *Seismic response and analysis of earth dams*, PhD thesis, Imperial College London.
- [30] Pelecanos, L., Kontoe, S., Zdravkovic, L., 2013, Numerical modelling of hydrodynamic pressures on dams, *Comput. and Geotech.*, 53, 68-62.
- [31] Pelecanos, L., Kontoe, S., Zdravkovic, L., 2015, A case study on the seismic performance of earth dams. *Géotechnique* 65 (11), 923-935
- [32] Pelecanos, L., Kontoe, S., Zdravkovic, L., 2016, Dam-reservoir interaction effects on the elastic dynamic response of concrete and earth dams. *Soil Dynamics and Earthquake Engineering* 82, 138-141
- [33] Potts, D. M., Zdravkovic, L., 1999, *Finite element analysis in geotechnical engineering: Theory*, Thomas Telford, London.
- [34] Saini, S. S., Bettess, P., Zienkiewicz, O. C., 1978, Coupled hydrodynamic response of concrete gravity dams using finite and infinite elements, *Earthq. Engrg. and Struct. Dyn.*, 6, 4, 363-374.
- [35] Tan, H., Chopra, A. K., 1996, Dam-Foundation Rock Interaction Effects in Earthquake Response of Arch Dams, *Earthq. Engrg. and Struct. Dyn.*, 122, 5, 528-538.
- [36] Timoshenko, S. P., Goodier, J. N., 1934, *Theory of Elasticity*, Mc-Graw Hill, New York.
- [37] Tsiatas, G., Gazetas, G., 1982, Plane-strain and shear-beam free vibration of earth dams, *Soil Dyn. and Earthq. Engrg.*, 1, 4, 150-160.
- [38] Von Estorff O., Antes H., 1991, On FEM-BEM coupling for fluid-structure interaction analyses in the time domain, *Int. J. for Num. Meth. Engrg.*, 31, 6, 1151-1168.
- [39] von Karman, T., 1933, Discussion on Water Pressures on Dams During Earthquakes, *Transactions, ASCE*, 98, 1, 434-436.
- [40] Westergaard, H. M., 1933, Water pressures on dams during earthquakes, *Transactions, ASCE*, 98, 1, 418-433.
- [41] Wilson, E. L., Khalvati, M., 1983, Finite elements for the dynamic analysis of fluid-solid systems, *Int. J. for Num. Meth. Engrg.*, 19, 11, 1657-1668.
- [42] Zangar, C. N., 1953, Hydrodynamic pressures on dams due to horizontal earthquakes, *Proc. Soc. Exp. Stress Anal.*, 10, 93-102.

## NOMENCLATURE

$a_0$	amplitude of harmonic acceleration load
$a(t)$	acceleration load time history
$E$	Young's elastic modulus
$ F $	amplification of acceleration
$G_w$	shear modulus of water
$H$	height of the dam

$I$	moment of inertia
$k$	stiffness
$K_d$	bulk modulus of the dam materials
$K_N, K_s$	normal and shear stiffness values of the interface elements
$K_w$	bulk modulus of water
$L$	length of the reservoir
$m$	mass
$S_a$	spectral acceleration